13

Hydrogenation of gadolinium thin films with a functional layer of niobium

© V.V. Matyukhov,[1,2] M.V. Makarova,[1] Yu.A. Salamatov,[1] V.V. Proglyado,[1] E.A. Tolmacheva,[1] E.A. Kravtsov[1,2]

[1] M.N. Mikheev Institute of Metal Physics, Ural Branch, Russian Academy of Sciences,
620108 Yekaterinburg, Russia
[2] Ural Federal University after the first President of Russia B.N. Yeltsin,
620002 Yekaterinburg, Russia
e-mail: vvmatyukhovimpuran@yandex.ru

Received April 24, 2025
Revised April 24, 2025
Accepted April 24, 2025

Controlled hydrogen saturation is a promising method for controlling the structural and magnetic properties of rare-earth metal thin films. Optimum conditions for hydrogenation of gadolinium thin films have been determined to obtain the required phases: a solid solution of hydrogen in gadolinium or gadolinium hydrides GdH_2 and GdH_3. It has been shown that hydrogenation of the gadolinium layer can be carried out both through a catalytic surface layer of platinum and through a functional niobium layer, without using noble metals. By analyzing the structural changes in the films, the processes of guiding of these two types in Gd thin films have been compared.

Keywords: X-ray diffractometry, X-ray reflectometry, hydrogen, gadolinium, gadolinium hydrides, thin film hydrogenation.

DOI: 10.61011/TP.2025.10.62081.69-25

Introduction

Heavy rare-earth metals (RE) have unique magnetic properties such as high magnetic moments per atom and a variety of types of magnetic ordering implemented in RE metals. Controlled hydrogen saturation is one of the promising techniques used to control structural, electronic and magnetic properties of rare-earth metals. Magnetic ordering in rare-earth metals is defined by RKKY interaction through conductivity electrons. Hydrogen saturation of rare-earth metals leads to a decrease in the number of electrons in the conduction band, having a significant effect on the RKKY interaction intensity and sign. Formation of alloys based on rare-earth metal hydrides provides a unique way to control mean magnetic moment, free carrier density and, consequently, magnetic properties of free carriers. Rare-earth metals are known to actively absorb hydrogen from ambient atmosphere, whilst, besides metal hydrides, solid solutions may be also formed depending on hydrogen pressure and temperature. It is known that, as the hydrogen concentration in a rare-earth metal increases, transitions between alpha phase (metal), beta phase (REH_2, semiconductor) and gamma phase (REH_3, dielectric) take place [1].

Gadolinium is a ferromagnetic rare-earth metal with the Curie temperature close to room temperature. Bulk gadolinium crystallizes into a HCP structure ($a = 3.629$ Å, $c = 5.760$ Å), it can interact with hydrogen to form HCP GdH_2 ($a = 5.268$ Å) and HCP GdH_3 ($a = 3.7218$ Å, $c = 6.7085$ Å) as well as a solid solution [2]. Moreover, gadolinium is a soft magnetic material with magnetocaloric effect, maximum values of which are achieved at the Curie temperature $T_C \approx 293$ K [3]. Study [4] provided a detailed investigation of the dependence of the Curie temperature on hydrogen concentration for bulk gadolinium, and showed that an increase in the Curie temperature was observed in GdH solid solutions with low hydrogen concentration.

Note that, while bulk gadolinium hydrogenation processes are relatively well studied at this point, systematic study of gadolinium thin films hasn't been performed, and the literature provides discrepant data. In contrast to bulk gadolinium samples, gadolinium thin films show anisotropic lattice expansion: expansion in the film plane is prevented by the influence of substrate and adjacent layers, while surface-normal expansion will be greater than that in the corresponding bulk gadolinium sample. Hydrogenation of ultrathin gadolinium films (units of monolayers) and relatively thick gadolinium films (hundreds of nanometers in thickness) is reported in the literature, and there is a few data concerning hydrogenation of films with intermediate thicknesses (units to tens of nanometers). In [5], during hydrogenation of 300 nm Gd film, it was found that, as the hydrogen pressure increased, transition from the hexagonal alpha phase of Gd to the cubic beta phase of GdH_2 and then to the cubic gamma phase of GdH_3 was observed. Hexagonal phase of GdH_3 was not detected. It was reported in [6,7] that after hydrogenation of 200 nm gadolinium film, a mixture of cubic phases of GdH_2 and GdH_3 semiconductors was formed in it. Hexagonal phase of GdH_3 wasn't detected either. On the other hand, in [8], reversible transition from the cubic phase of GdH_2 to the hexagonal phase of GdH_3 was observed during hydrogenation of 40 nm and 80 nm gadolinium thin films (reversible transition was observed after holding the film in air outside the chamber for several hours). Finally, in [9], a hexagonal phase was obtained at high temperatures in 500 nm gadolinium films

coated by a catalytic Ni layer. Typically, a hexagonal phase wasn't observed in films without a catalytic layer.

Magnetic properties of gadolinium hydride thin films also remain underinvestigated. In [10,11], it is concluded that gadolinium thin film in transition to the beta and gamma phases during hydrogenation remains ferromagnetic with a decreased Curie temperature and saturation magnetization due to the presence of hydrogen-unsaturated regions and inhomogeneous hydrogen distribution over the film volume. Magnetism of gadolinium hydride thin films has been poorly explored and should be investigated in terms of its dependence on hydrogen concentration, and the presence of GdH_2 and/or GdH_3.

For rare-earth metal film hydrogenation, a catalytic layer is generally applied to facilitate hydrogen molecules dissociation into radicals penetrating deep into the film. As a catalytic layer, noble metals are used: gold, platinum, palladium, etc. [12] They enable hydrogenation at room temperature and low hydrogen pressures, however, limit the sample temperature stability and are expensive. Applicability of Ni as a catalytic layer was discussed in [13]. But Ni falls far behind noble metals in terms of catalytic properties and, being a ferromagnetic material with the Curie temperature of 360 °C, hinders the investigation of magnetic systems. Recently, we have discussed whether niobium could be used as a functional layer for hydrogenation and established conditions for formation of solid solution and/or niobium hydride [14].

Hydrogen dissociation processes proceed differently on the niobium surface and noble metal surfaces. Hydrogen may either loose its electron, thus, turning into a proton, or accept an electron to form H^-. It has been found that hydrogen in hydrides of transition metals such as palladium and platinum was in the form of proton [15], at the same time, rare-earth metal hydrides contained negatively charged hydrogen ions [16]. Since proton mobility in metals is much higher than negative hydrogen ion mobility, then hydrogenation processes in Gd films with Pt catalytic layer and Nb functional layer on the surface will flow differently. Functional layer on the substrate is required to match lattice parameters, improve adhesion and prevent interpenetration of substrate and film atoms. Being placed on top of the structure, it protects the structure against oxidation in air. Hydrogenation of gadolinium films coated with the Pt catalytic layer will flow quickly even at room temperature, moreover, formation of both gadolinium dihydride and trihydride may be expected. Hydrogenation of gadolinium film without a catalytic layer will flow quite slowly and heating of the sample will be required. At the same time, formation of solid solution may be expected. The purpose of the study is to perform comparative determination of the best hydrogenation conditions for gadolinium nanometer films with the Nb functional layer and Pt catalytic layer on the surface to form solid solutions and gadolinium hydrides. Conditions, in which the hexagonal phase of gadolinium trihydride in such films, are studied.

1. Experiment

Gd films without a catalytic layer were grown on single-crystal silicon substrates with the (100) orientation, with Nb buffer and covering layers: Si//Nb(50 Å)/Gd(250 Å)/Nb(50 Å). Gd layers with the Pt catalytic layer were grown on sapphire single-crystal substrates with the $(1\bar{1}02)$ orientation, the sample structure is Al_2O_3//Nb(250 Å)/Gd(375 Å)/Nb(250 Å)/Pt(30 Å). Synthesis was performed by magnetron sputtering of high purity targets by argon plasma using the ULVAC MPS 4000 C6 system at the Institute of Metal Physics, Ural Branch, Russian Academy of Sciences (Yekaterinburg). Sputtering was performed at room temperature; the base vacuum level in the growth chamber was $5 \cdot 10^{-7}$ Pa, the argon pressure was ~ 0.1 Pa and the growth rate was ~ 0.5 Å/s.

Hydrogenation was carried out in a horizontal quartz chemical reactor placed in a resistance furnace. The sample was placed on a horizontal quartz table without additional clamping. The reactor was evacuated to less than 100 Pa, then purged with 1 l/min argon flux for 1 min to remove residual gases. Then the sample was heated in vacuum to an operating temperature within 190−360 °C. On reaching the operating temperature, the reactor was filled with pure molecular hydrogen to reach atmospheric pressure. Holding time in each of the processes was 1 h, with hydrogen continuously pumped through the reactor at 1 l/min to avoid plasma-forming gas depletion and hydrogen partial pressure drop. Upon completion of the process, hydrogen was cut off, the furnace was turned off and furnace clamshells were opened for quicker cooling down. Residual hydrogen was drained, and the reactor was purged with Ar following the same procedure as before the process. The reactor was filled with Ar to atmospheric pressure, further cooling down was performed in a slow Ar flux 0.1 l/min, to avoid possible entry of atmospheric air into the reactor and oxidation of the hot sample. Samples were removed from the reactor at a temperature below 50 °C.

Structural modifications, multilayer structure quality, layer thicknesses and degree of imperfection of interlayer boundaries were evaluated on the basis of X-ray diffraction and reflectivity data. X-ray measurements were performed using the PANalytical Empyrean Series 2 laboratory diffractometer using CoK_α line radiation at 1.79 Å in the parallel beam configuration. A parabolic reflector based on a W/Si superlattice was used in the primary beam to suppress the CoK_α radiation line together with formation of a parallel beam. X-ray measurements were performed in the mirror configuration $\Theta - \Theta$. For reflectivity measurements, a 1/16° divergence slit was used. The beam height was 0.16 mm. A plane-parallel collimator with a plane graphite monochromator and collimating slit with an equatorial aperture of 0.1 mm was used at the secondary beam. Reflectograms were processed using the commercial PANalytical X'Pert Reflectivity software. X-ray measurements were performed and repeated long after extraction of the samples from the

reactor, no changes were observed on the X-ray diffraction patterns.

2. Results and discussion

X-ray diffraction measurement demonstrate formation of axial textures of BCC niobium (110) and HCP gadolinium (0002) in the samples, which corresponds to previously obtained data [17,18]. The specified lattice planes of the layers are parallel to the substrate plane. Position of the gadolinium (0002) reflection was used to evaluate the Gd lattice parameter variation during hydrogenation. Figure 1 shows the X-ray diffraction data for the original gadolinium thin film with buffer and protective niobium layers and of these films after hydrogenation at the ambient pressure and various process temperatures. At 190 °C, the lattice parameter c_{Gd} slightly decreases due to stress relaxation in a thin film during temperature treatment. No any perceptible hydrogen penetration into the system occurs yet at this temperature. Within 190–240 °C, increase in the gadolinium lattice parameters is observed and demonstrated by the shift of the Bragg peak of Gd (0002). While the niobium lattice remains unchanged, suggesting that hydrogen has moved from the niobium to the gadolinium layer. At 240 °C, the gadolinium lattice parameter varied by 0.026 Å (0.4 %), indicating that a hydrogen solid solution has formed in gadolinium.

Significant structural modifications take place with further increase in the hydrogenation temperature: hydrogen penetrating into the gadolinium layer reacts with gadolinium to form GdH_2, which is indicated by the (0002) Gd peak asymmetry. Interpretation of these results was hindered by the fact that the Bragg peak position of (0002) Gd and (111)GdH_2 differ from positions typical of the bulk

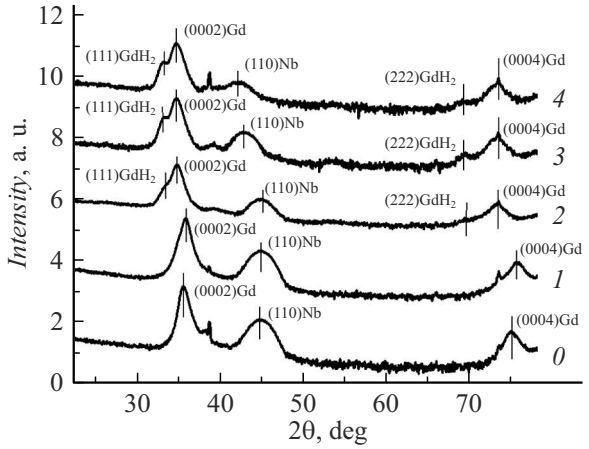

Figure 1. X-ray diffraction patterns of the Si//Nb(50 Å)/Gd(250 Å)/Nb(50 Å) sample subjected to hydrogenation in various conditions: *0* — original state, *1* — at 190 °C, *2* — at 247 °C, *3* — at 260 °C, *4* — at 310 °C. Intensity was shown on a logarithmic scale, curves are shifted vertically for clarity.

sample measured in PowderCell [19]. This is due to the inevitable presence of stresses in the metal thin film induced by incomplete match between the lattice parameters of the substrate and deposited material. To ensure correct interpretation, second-order peaks of (0004) Gd, (222) GdH_2 were also reviewed. For verification, the lattice parameters were calculated and compared using the angular positions of first-order and second-order peaks. For example, at 255 °C, we have: $a_{(0002)} = (6.049 \pm 0.009)$ Å and $a_{(0004)} = (6.046 \pm 0.004)$ Å; $a_{(111)} = (5.444 \pm 0.009)$ Å and $a_{(222)} = (5.448 \pm 0.004)$ Å. The parameters for different orders coincide within the permissible error, suggesting that peaks were interpreted correctly and GdH_2 occurrence time was determined correctly as well.

At 260 °C, the peak from gadolinium remains absolutely unchanged, however, the (111) GdH_2 peak becomes more intense. It may be concluded that excess hydrogen insoluble in the lattice forms dihydride, and the amount of solid solution doesn't decrease. Niobium at this temperature also starts interacting intensively with hydrogen, which, according to [20,21], leads to significant expansion of the lattice in the sample plane and formation of niobium hydrides. The X-ray diffraction data may be used to establish that the niobium lattice parameter a_{Nb} increases by 0.15 Å and a small peak occurs and may be interpreted as a reflection from (111) NbH_2. A low narrow peak at approx. 38.5° isn't interpreted as a structural peak and is probably associated with a large-scale substrate defect because it disappears at particular sample positions on the diffractometer table. Identical results for the NbH_2 formation process were addressed in [14].

Further increase in the hydrogenation temperature has no any effect on the condition of gadolinium films and the resulting GdH_2. The Nb peak continues shifting towards small angles, indicating that niobium continues to be saturated with hydrogen, thus increasing the concentration of NbH_2. This behavior corresponds to the findings of our previous work [14]. Niobium dihydride presumably reduces the catalytic activity of the layer, allowing hydrogen molecules to dissociate into radicals and, thus, becomes a „barrier“ for hydrogen.

The plotted dependences of the Gd and GdH_2 lattice parameters on temperature (Figure 2) clearly show that as the hydrogenation temperature increases to 255 °C, the gadolinium lattice parameter increases, and then stops changing. This may indicate that maximum hydrogen saturation occurred at 255 °C, i.e. the gadolinium dihydride formation temperature. Decrease in the crystal lattice parameter at the start of the process is caused by stress relaxation in the film during annealing. As expected, the GdH_2 lattice parameter isn't subjected to any significant changes as the temperature grows.

According to the X-ray reflectivity data (Figure 3), the original Gd layer thickness is 24.8 nm, and density is 7.90 g/cm^3 (in accordance with the Gd density in thin films [22]). Broad oscillations at the end of the reflectogram

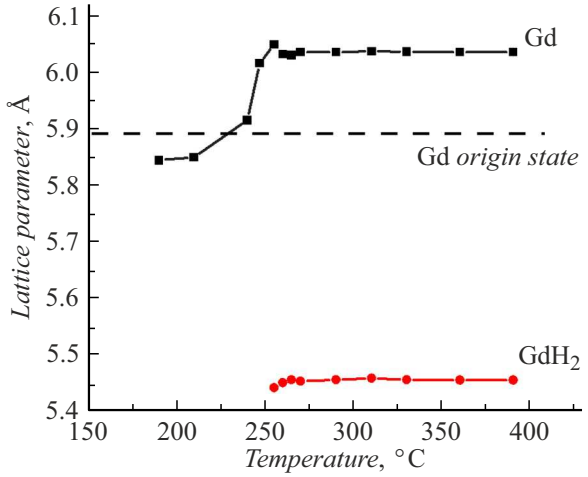

Figure 2. Dependence of the gadolinium and GdH_2 lattice parameters on the hydrogenation temperature. The dashed line shows the lattice parameter in the Gd layer before hydrogenation.

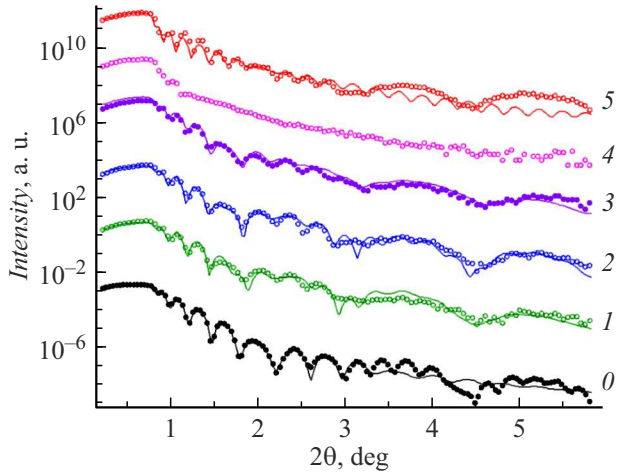

Figure 3. X-ray reflectivity curves (symbols) and processing results (solid lines) for the Si//Nb(50 Å)/Gd(250 Å)/Nb(50 Å) film at various hydrogenation temperatures: *0* — original state, *1* — at 190 °C, *2* — at 210 °C, *3* — at 240 °C, *4* — at 247 °C, *5* — at 265 °C. The curves are shifted vertically for clarity.

are associated with the presence of Nb_2O_5 approximately 2.9–3.4 nm in thickness on the film surface. Below the hydrogenation temperature of 240 °C, gadolinium density decreases to 7.45 g/cm^3 and thickness increases to 25.4 nm due to the formation of solid solution (Figure 4). At a hydrogenation temperature above 255 °C, a rapid growth of the Gd layer thickness is observed as the density decreases, which corresponds to the X-ray diffraction data and confirms the formation of GdH_2 and increase in the concentration of hydrogen solid solution in gadolinium. Note that the reflectogram obtained for the sample hydrogenated at 247 °C has a smooth intensity decrease without any noticeable oscillations. This indicates a significant increase in the layer interface roughness, which may be attributed to the start of GdH_2 formation (according to the diffraction data, this occurs exactly at this temperature). It is impossible to determine the Gd layer thickness using such reflectivity curve. As the temperature further increases, the amount of hydride increases, layer interfaces are partially restored due to diffusion. Oscillations corresponding to a multilayer structure occur on the reflectogram again.

We now analyze the results for the sample with the catalytic platinum layer. Review [1] showed effective utilization of a catalytic platinum layer for hydrogenation at 10^6 Pa. We have studied how low pressure would affect the hydrogenation results, therefore hydrogenation was carried out at room temperature, the process pressure varied from 240 Pa to 15 kPa. Figure 5 shows X-ray diffraction patterns of the sample after the processes at various hydrogen pressures.

The sample contains gadolinium dihydride already in the original state because the catalytic layer dissociates hydrogen from atmospheric air and facilitates hydrogen penetration into the system. Bragg peaks of (1000) Gd, (0002) Gd and (111) GdH_2 are clearly distinguished on the diffraction pattern. At 240 Pa, the (111) GdH_2 peak becomes more intense, however, hydrogen solid solution also remains in gadolinium. As the hydrogen concentration increases, gadolinium obviously transforms into gadolinium dihydride, which affects the disappearance of peak (1000) and significant decrease in the intensity of the (0002) peak. Further increase in pressure up to 295 Pa leads to full transition of gadolinium into GdH_2 (diffraction peaks corresponding to pure gadolinium disappear) and appearance of hydrogen solid solution in niobium and NbH_2, which is indicated by occurrence of a corresponding reflection. At 320 Pa, GdH_3 is formed, with its amount becoming larger than the amount of GdH_2, which is indicated by the higher intensity of the Bragg peak of (0002) GdH_3. Further increase in pressure results in further increase in the amount of GdH_3 and decrease in the amount of GdH_2. This trend is maintained up to 15 kPa, where only GdH_3 remains, no structural modifications are observed any longer at higher pressures.

Dependence of the lattice parameter on the process pressure is shown in Figure 6. As can be noted, lattice parameters remain virtually unchanged regardless on whether it is metal or hydride. However, note that only one of gadolinium hydrides as well as a set of gadolinium hydrides may be formed at different hydrogenation pressures. Only hydrogen solid solution in gadolinium cannot be formed for this system.

According to the X-ray reflectivity data (Figure 7), it was found that the original samples had a thickness of 37.5 nm, and a density of 7.90 g/cm^3 (in accordance with the Gd density in thin films [22]). Increase in the hydrogen pressure causes an increase in the layer thickness and RMS roughness of Gd/Nb layer interfaces, and a decrease in Gd density. At 295 Pa, the sample density becomes 7.14 g/cm^3, which may suggest full transition of metallic gadolinium into GdH_2 because the resulting density is close

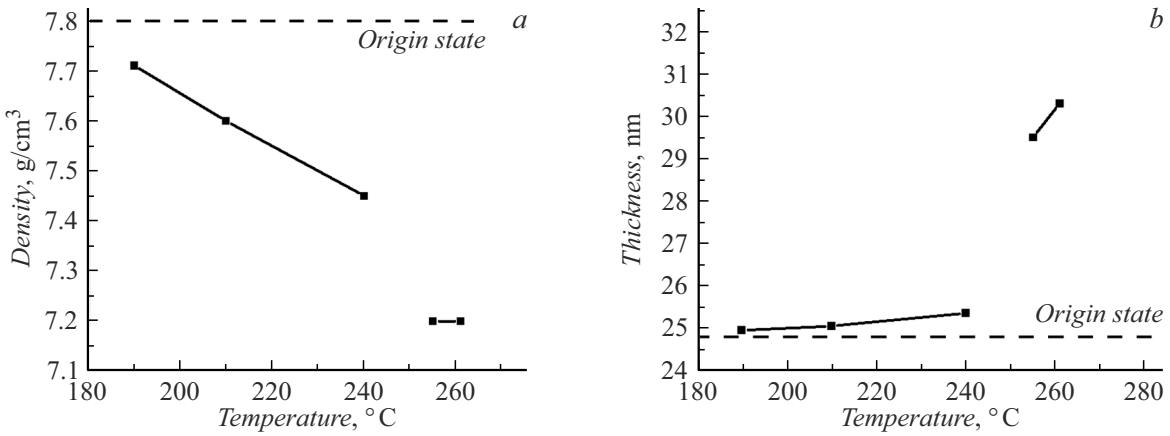

Figure 4. Dependences of Gd layer density (*a*) and thickness (*b*) variations at various hydrogenation temperatures. The gaps correspond to 247 °C, at which the reflectivity data was not processed. The dashed line shows Gd layer density and thickness before hydrogenation.

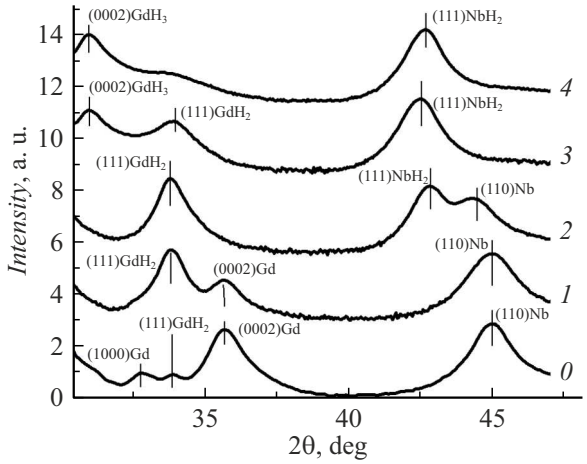

Figure 5. X-ray diffraction patterns of gadolinium thin film with a buffer niobium layer and catalytic platinum layer subjected to hydrogenation in different conditions: *0* — original state, *1* — at 240 Pa, *2* — at 295 Pa, *3* — at 320 Pa, *4* — at 15 kPa during 1 h. Intensity is plotted on the logarithmic scale, curves are shifted vertically for clarity.

to the GdH_2 density of 7.11 g/cm^3. Thickness increases by 4.6 nm in this case (Figure 8). At 1.33 kPa, the thickness increases significantly and becomes equal to 53.7 nm, which is caused by formation of GdH_3. As the pressure further increases, the thickness keeps increasing and the density keeps decreasing. At 15 kPa, the density is 6.5 g/cm^3, the layer thickness is 75 nm. No further structural modifications are observed as the pressure increases. Layer density quite closely corresponds to the gadolinium trihydride density (reference values is 6.61 g/cm^3) and this confirms the X-ray diffraction results indicating that only GdH_3 remained in the system.

Comparing the hydrogenation processes flowing in Nb/Gd/Nb systems with and without the catalytic platinum layer, the following typical features may be noted. Hydrogenation of the film without the Pt layer takes place much slower, providing a theoretical opportunity to reach the required hydrogen concentration in the system. The sample with the catalytic layer starts saturating with hydrogen already in normal conditions, that's why hydrogen solid solution cannot be achieved in gadolinium without a hydride impurity. This phase likely occurs for a very short time after the first contact between the synthesized sample and air. However, it can be easily obtained in the system without a catalytic layer. Thus, when it is necessary to perform intense gadolinium hydrogenation with formation of a mixture of hydrides or only trihydride, a catalytic layer (platinum, palladium is also possible) shall be preferably used. On the contrary, it is better to perform precision hydrogenation directly through niobium without using a catalytic layer. Solid solution can be easily obtained in this case. The hydrogen saturation process may be also slowed down, if necessary, using a graphene layer as an additional barrier [14].

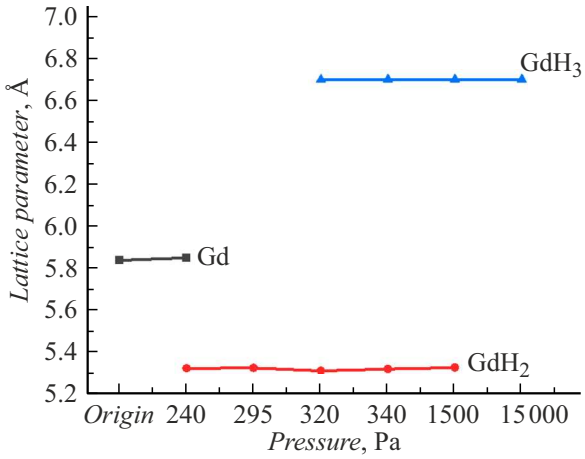

Figure 6. Dependence of Gd, GdH_2, GdH_3 lattice parameters on the hydrogenation pressure for the sample without a catalytic layer.

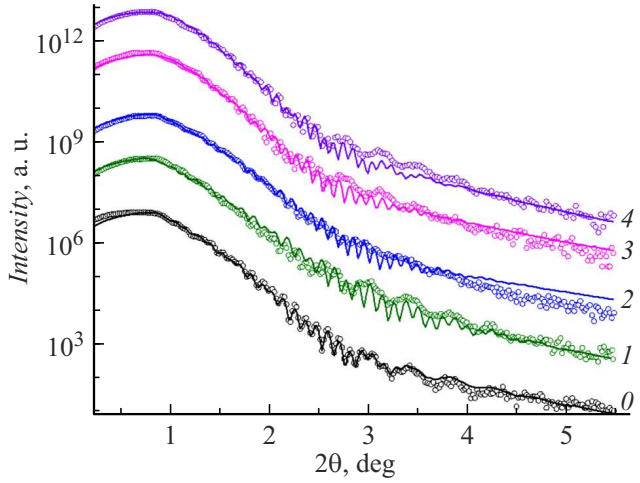

Figure 7. X-ray reflectivity curves (symbols) and processing results (solid lines) for the Al_2O_3//Nb(250 Å)/Gd(375 Å)/Nb(250 Å)/Pt(30 Å) film at various hydrogenation pressures: *0* — original state, *1* — at 240 Pa, *2* — at 295 Pa, *3* — at 320 Pa, *4* — at 1.33 kPa. The curves are shifted vertically for clarity.

The general hydrogenation process trend is common for both types of samples. Hydrogen solid solution is first formed in gadolinium, resulting in lattice expansion. Then, formation of GdH_2 starts, and this phase coexists with the solid solution. Then, only GdH_2 remains, and GdH_3 also occurs as the pressure further increases. Finally, GdH_2 fully transforms into GdH_3 and only this phase remains. For the sample without a catalytic layer, GdH_3 wasn't observed, but probably may be obtained through a considerable increase in the holding time because the main difference between the studied systems is in the hydrogenation process rate.

Conclusion

It has been shown before that niobium thin films had high hydrogen absorption capacity even without a catalytic noble metal (Pd, Pt) layer. The study demonstrates that the niobium layer also facilitates hydrogen penetration into the underlying gadolinium layer and allows obtaining both a pure hydrogen solid solution and a mixture of solid solution and GdH_2.

According to the X-ray diffraction and reflectivity results for the Nb/Gd/Nb system, structural modifications of the gadolinium layer with hydrogen saturation were analyzed and conditions allowing the necessary finite states to be obtained were determined. Thus, it has been found that below 240 °C the gadolinium layer didn't undergo any changes and was resistant to hydrogen atmosphere. In the range from 240 °C to 247 °C, only hydrogen solid solution in gadolinium is formed, which is important for magnetic structure modification. With further increase in the temperature up to 261 °C, hydrogen concentration in the gadolinium layer increases, however, GdH_2 is formed, which may be undesirable for magnetic state control. Formation of GdH_3 in this system was not observed. Thus, the best hydrogenation conditions were determined to obtain a hydrogen solid solution in gadolinium with the desired lattice parameter, but to avoid formation of hydrides at the same time. For this, any catalytic noble metal layer and low gas pressures are not required, but a certain process temperature must be maintained.

It has been also found that maximum hydrogen saturation of the gadolinium layer was observed at 261 °C, i.e. structural properties of gadolinium stopped changing. This effect is probably defined by the time when NbH_2 is formed. NbH2 prevents hydrogen molecule dissociation and further penetration into the underlying layers.

For the sample with the catalytic platinum layer, Nb/Gd/Nb/Pt, it has been found that GdH_2, besides metallic Gd, was already present in the original state, suggesting

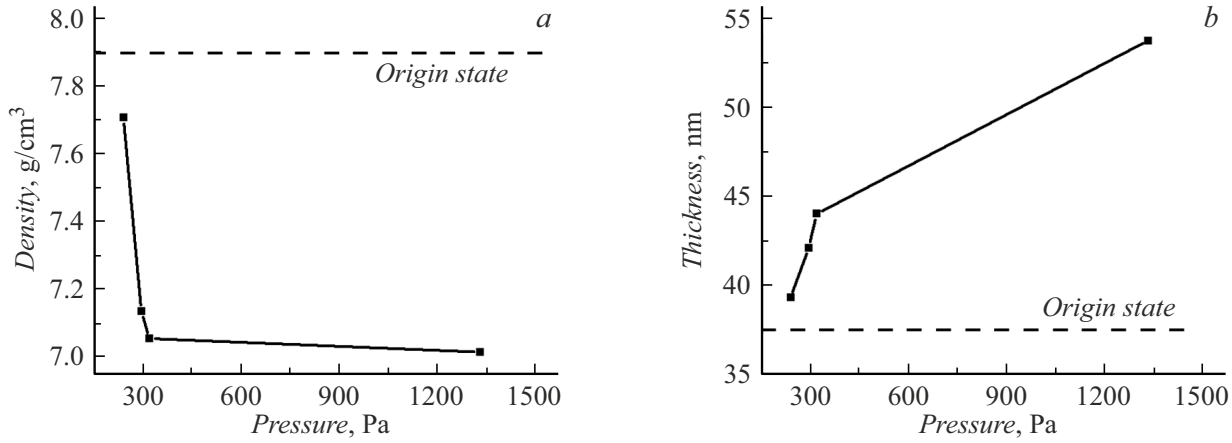

Figure 8. Dependences of Gd layer density (*a*) and thickness (*b*) variations in the sample with the catalytic layer at various hydrogenation pressures. The dashed line shows Gd layer density and thickness before hydrogenation.

hydrogen penetration into the thin film from the air. Gradual pressure increase makes it possible to obtain each of the gadolinium hydrides separately as well as a set of gadolinium hydrides. But the hydrogen solid solution in gadolinium cannot be obtained without hydrides. At sufficiently high hydrogen pressure, a system consisting of a mixture of cubic GdH_2 and hexagonal GdH_3 phases can be formed, where the latter is predominant. Transition into the cubic phase in films over time was not observed, the phase composition remained stable for a considerable period of time after sample removal from the reactor.

Thus, depending on the tasks, hydrogen solid solution in gadolinium or each of the gadolinium hydrides separately may be obtained by choosing a system with or without a catalytic layer and appropriate hydrogenation process variables.

The results are needed to make necessary structural modifications during hydrogenation of layered systems and superlattices with gadolinium, and to establish correlation between the magnetic properties, structure and degree of hydrogenation of gadolinium thin films.

Funding

This study was supported by grants provided by the Russian Science Foundation (project №. 24-12-20024) and the Sverdlovsk region (project №. 2-25-OG). The work was performed using the equipment of the Collaborative Access Center „Testing Center of Nanotechnology and Advanced Materials“ Institute of Metal Physics, Ural Branch of RAS.

Conflict of interest

The authors declare no conflict of interest.

References

[1] P. Vajda. In *Handbook on the Physics and Chemistry of Rare Earths*, ed. by K.A. Gschneidner, L. Eyring (Elsevier, North-Holl. Amsterdam, 1995), v. 20, p. 207.
[2] I.V. petryanov-Sokolov. *Populyarnaya biblioteka khimicheskikh elementov* (Nauka, M., 1977) (in Russian)
[3] A.P. Kamantsev, V.V. Koledov, V.G. Shavrov, L.N. Butvina, A.V. Golovchan, V.I. Valkov, B.M. Todris, S.V. Taskaev, FMM, **123** (4), 448 (2022) (in Russian). DOI: 10.31857/S0015323022040064
[4] E.A. Tereshina, S. Khmelevskyi, G. Politova, T. Kaminskaya, H. Drulis, I.S. Tereshina. Sci. Rep., **6** (1), 22553 (2016). DOI: 10.1038/srep22553
[5] E. Shalaan, K.H. Ehses, H. Schmitt. J. Mater. Sci., **41**, 7454 (2006). DOI: 10.1007/s10853-006-0798-9
[6] A. Marczyńska, S. Pacanowski, B. Szymański, L. Smardz. Acta Phys. Polon., **133**, 624 (2018). DOI: 10.12693/APhysPolA.133.624
[7] M. Wachowiak, L. Smardz. Intern. J. Hydrogen Energy, **48**, 26840 (2023). DOI: 10.1016/j.ijhydene.2023.03.282
[8] P. Tessier, D. Fruchart, D. Givord. J. Alloys Comp., **330**, 369 (2002). DOI: 10.1016/S0925-8388(01)01639-5
[9] H. Hirama, M. Hayakawa, T. Okoshi, M. Sakai, K. Higuchi, A. Kitajima, A. Oshima, S. Hasegawa. J. Cryst. Growth., **378**, 356 (2013). DOI: 10.1016/j.jcrysgro.2012.12.175
[10] V. Leiner, M. Ay, H. Zabel. Phys. Rev., **70**, 104429 (2004). DOI: 10.1103/PhysRevB.70.104429
[11] Y. Manassen, H. Realpe, D. Schweke. J. Phys. Chem. C, **123** (18), 11933 (2019). DOI: 10.1021/acs.jpcc.9b00932
[12] L.J. Bannenberg, B. Boshuizen, F.A. Nugroho, H. Schreuders. ACS Appl. Mater. Interfaces, **13** (44), 52530 (2021). DOI: 10.1021/acsami.1c13240
[13] I.A. Likhachev, I.A. Subbotin, Yu.M. Chesnokov, D.I. Devyaterikov, O.A. Kondrat'ev, A.A. Ryzhova, Yu.A. Salamatov, M.A. Milyaev, A.L. Vasil'ev, E.A. Kravtsov, E.M. Pashaev. Phys. Metals Metallogr., **124** (12), 1224 (2023). DOI: 10.1134/S0031918X23602202
[14] Yu.A. Salamatov, D.I. Devyaterikov, M.V. Makarova, V.V. Matyukhov, Yu.S. Ponosov, V.V. Proglyado, E.A. Tolmacheva, E.A. Kravtsov. ZhTF, **95** (3), 615 (2025) (in Russian). DOI: 10.61011/JTF.2025.03.59869.360-24
[15] B. Baranowski. Physica B, **265**, 16 (1999). DOI: 10.1016/S0921-4526(98)01309-X
[16] R.C. Brouwer, R. Griessen, Phys. Rev. Lett., **62**, 1760 (1989). DOI: 10.1103/PhysRevLett.62.1760
[17] D.I. Devyaterikov, V.O. Vas'kovsky, V.D. Zhaketov, E.A. Kravtsov, M.V. Makarova, V.V. Proglyado, E.A. Stepanova, V.V. Ustinov. Phys. Metals Metallogr., **121**, 1127 (2020). DOI: 10.1134/S0031918X20120042
[18] L. Helmich, M. Bartke, N. Teichert, B. Schleicher, S. Fähler, A. Hütten. AIP Adv., **7**, 056429 (2017). DOI: 10.1063/1.4977880
[19] W. Kraus, G. Nolze. J. Appl. Cryst., **29**, 301 (1996). DOI: 10.1107/S0021889895014920
[20] P.M. Reimer, H. Zabel, C.P. Flynn, J.A. Dura. J. Cryst., **127**. 643 (1993). DOI: 10.1016/0022-0248(93)90701-W
[21] T. Matsumoto, J. Eastman, H.K. Birnbaum. Scripta Met., **15**, 1033 (1981).
[22] J.W. Arblaster. *Selected Values of the Crystallographic Properties of the Elements* (ASM International, 2018)

Translated by E.Ilinskaya

Translated by E.Ilinskaya